International Journal on Advanced Science Engineering Information Technology

Vol.12 (2022) No. 5
ISSN: 2088-5334

Graduating Mortality Rates by Mixture of Pareto, Loglogistic, and Two Weibull Distributions using Bayesian Method

Christian Evan Chandra [a], Sarini Abdullah [a,*]

[a] Department of Mathematics, University of Indonesia, Kampus Baru UI Depok, 16424, Indonesia
Corresponding author: *sarini@sci.ui.ac.id

***Abstract*— Mortality rates are important in conducting the pricing and valuation of life insurance policies. Raw values are usually wiggly to plot, and practitioners often graduate them to obtain smoothness. Current mortality models have problems related to the goodness of fit, interpretability, and usability without implementing other actuarial assumptions for fractional ages. This study proposes a mixture of Pareto, log-logistic, and two Weibull distributions with eleven parameters to graduate mortality rates. Lifespan covered are whole life, including childhood, adolescence, senescence, and the late elderly's phase. We adjusted the parameterization to improve the ease of model's interpretability right after obtaining the value of estimates. Prior distributions of the parameters and sampling model form for the data are also proposed to estimate the parameters' value using the Bayesian method with Gibbs sampling. High values of coefficient of determination produced by model fit into several data support the graphical evidence to show the model's goodness of fit and best fit occurs for the life table of Israeli males in 1987. Gelman-Rubin statistic is also very close to one and shows fast convergence in estimating the parameters. Based on the results, obtaining the best and worst estimates of newborn survival probabilities is possible. We also showed that this model could be implemented on annual and abridged mortality rates.**

***Keywords*— Bayesian method; mixing distribution; mortality graduation; newborn survival probabilities; parametric model.**

Manuscript received 13 May 2021; revised 24 Jun. 2021; accepted 3 Aug. 2021. Date of publication 31 Oct. 2022.

I. INTRODUCTION

There are two main uncertainties in conducting insurance industries, demographic uncertainty and investment uncertainty. Demographic uncertainty relates to the mortality rates, especially when the number of policyholders in the portfolio tends to be small and the policies have a very high sum at risk [1]. Mortality rates are used as a basis in the valuation of employee pensions and other benefit plans and pricing or reserving life insurance products [2]. It is a model that generally explains two conditions: current mortality and improvement trend. When it is easy and fast enough to obtain the most recent data, the former is getting much concern.

Raw data of mortality rates usually produce wiggly plots, and practitioners often choose to have a smoothing process, also known as graduation. For example, the implementation of P-splines, Greville's cubic polynomials (as implemented in Japanese Standard Mortality Table 2018 [3]), or the Whittaker-Henderson method (as implemented in Canadian Pensioners' Mortality table 2014 and 4th Indonesian Mortality Table [4]) could be employed. Another approach that could be considered is fitting the mortality rates on parametric mortality models, and this approach helps practitioners to understand the drivers of mortality and intuitively explain those drivers.

De Moivre model using one parameter is simple, but the constant value of hazard rate at age x (μ_x) is not suitable for older ages. Gompertz model was initially formed using a formula with two age-dependent parameters to express exponentially increasing mortality rates. This model is then improved by adding age-independent parameters, which gave accurate predictions for ages 30-80 years [5] and plausibly extrapolate in many actuarial works. However, this model did not fit well for ages under 20 [6].

Pareto found that his distribution was a good fit for the first twenty years of life in Switzerland and Bavaria but could not be used for extrapolation [6]. His later work [6] provided a good fit for the age between 0 and 88 years to explain the number of survivors at age x, denoted as N(x), in Italian data during the years 1881-1883, which is written as (1). However, it does not give us an intuitive way to understand the mortality characteristics of the population.

$$N(x) = \frac{1.548}{(x+2)^2} + 0.613 - 0.0021x - 0.0000412x^2 - 0.13e^{-0.0046(x-82)^2} \quad (1)$$

Later, Heligman and Pollard [7] also constructed their model to cover the whole life span. It consists of eight parameters, can capture accident humps, provides a good fit for all ages [8], and every parameter has an intuitive explanation. However, it is often overparameterized [9]. This model cannot produce the hazard rate, resulting in the inability to calculate the value of complete life expectancy without implementing other actuarial assumptions in fractional ages (for example, the Balducci assumption). The Siler model is an alternative model that produces good fits [10] but fails to capture accident humps.

Bebbington et al. [11] mixed flexible Weibull and reduced additive Weibull survival functions to obtain the hazard rate and produce better interpretability than Gompertz and Makeham models but requires further complex mathematical derivation for the explanations. Beer and Janssen constructed a compression and delay (CoDe) mortality model that can explain five stages in life by eleven parameters, but it only provides the value of annual mortality rates [12]. Therefore, we cannot calculate the value of complete life expectancy without other actuarial assumptions involved. Mazzuco et al. [9] mixed skew bimodal normal and half-normal distributions to obtain a flexible model that can fit data with and without accident hump, but the interpretation of the parameters is not intuitive enough.

In this study, we propose the mix of Pareto, log-logistic, and two Weibull distributions (later named as PL2W model) to graduate mortality data with interpretable parameters in an intuitive way and good statistical fit. Implementing the Bayesian method, we propose prior distribution for the parameters of interest. A Bayesian method is chosen due to its ability to incorporate prior knowledge, reliability of small data, and producing more realistic and intuitive interval estimates than the frequentists' methods [13]–[17].

II. Material and Method

In this section, we describe baseline distributions that were used to construct our model. After the model is constructed, we provide intuitive interpretation and determine appropriate prior distributions for every parameter. We propose to fit the model using the Bayesian method and to calculate the best and the worst estimate of newborn survival probabilities. The flowchart summarizes the summary of the process in Fig. 1.

A. Overview of Pareto, Loglogistic, and Weibull Distributions

Some distributions have a relatively simple function of hazard rate, survival function, probability density function, and mean (first moment), but some others do not. Having long tail and flexible distribution properties that produced satisfactory model fits in various data as shown in, for example, [18]–[21] for Pareto, [22]–[24] for log-logistic, and [25]–[27], we consider these distributions for this study.

1) Pareto Distribution: As mentioned in Section 1, Pareto successfully fitted his distribution for the population aged under 20. We considered two parameters of Pareto distribution as provided in [28]. If X is Pareto distributed with parameters α and θ, the hazard rate, the survival function, and the first moment of X could be written as (2), (3), and (4), respectively. The hazard rate is a monotone decreasing function of x and is suitable to explain mortality rates for the young population, especially in childhood. Moreover, the hazard rate is a monotone increasing function of α and a monotone decreasing function of θ. Consequently, the survival function and the first moment are a monotone increasing function of θ and a monotone decreasing function of α.

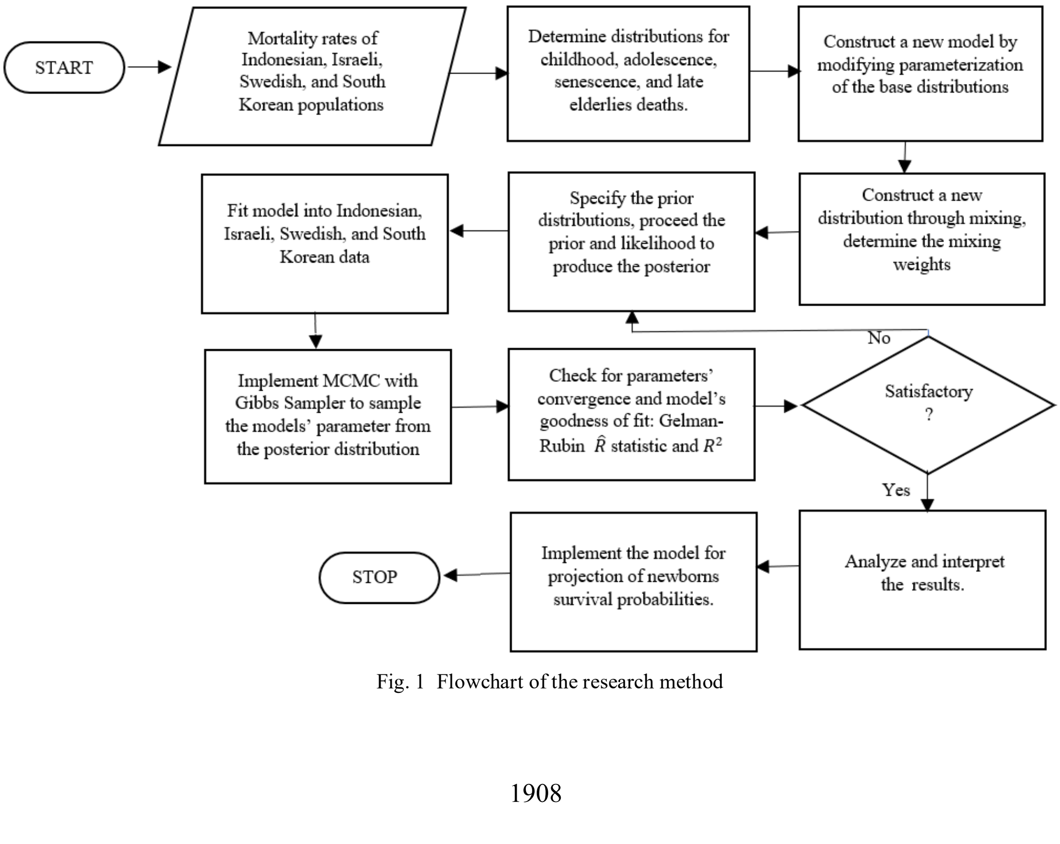

Fig. 1 Flowchart of the research method

$$h(x) = \frac{\alpha}{x+\theta}, \alpha > 0, \theta > 0 \quad (2)$$

$$S(x) = \left(\frac{\theta}{x+\theta}\right)^{\alpha}, \alpha > 0, \theta > 0 \quad (3)$$

$$E(x) = \frac{\theta}{\alpha-1}, \alpha > 1, \theta > 0 \quad (4)$$

2) Loglogistic Distribution: If there is an accident hump in the mortality rates, we need hump-shaped distribution to explain it. We considered log-logistic distribution over lognormal distribution for a more tractable survival function. If X is log-logistic distributed with parameters α and λ, the hazard rate, the survival function, and the first moment of X could be written as (5), (6), and (7), respectively.

$$h(x) = \frac{\alpha\lambda x^{\alpha-1}}{1+\lambda x^{\alpha}}, \alpha > 0, \lambda > 0 \quad (5)$$

$$S(x) = \frac{1}{1+\lambda x^{\alpha}}, \alpha > 0, \lambda > 0 \quad (6)$$

$$E(X) = \frac{\pi \csc\left(\frac{\pi}{\alpha}\right)}{\alpha\lambda^{\frac{1}{\alpha}}}, \alpha > 1, \lambda > 0 \quad (7)$$

The characteristic of the hazard rate depends on the value of α. For $\alpha \leq 1$, the hazard rate is a monotone decreasing function of x. For $\alpha > 1$, the hazard rate increases initially to its peak at the time $\left(\frac{\alpha-1}{\lambda}\right)^{\frac{1}{\alpha}}$ then decreases as x approaches infinity with zero as the asymptote. To fit the condition of the accident hump, later, we restrict the value of α to be greater than one. By limiting our attention to $x \geq 1$, the hazard rate is a monotone increasing function of both α and λ.

3) Weibull Distribution: Makeham model states the force of mortality as a monotone increasing function of age. Therefore, we need an alternative distribution with a similar characteristic, and the Weibull distribution fulfills that need with certain limitations. If X is Weibull distributed with parameters α and λ, the hazard rate, the survival function, and the first moment of X could be written as (8), (9), and (10), respectively.

$$h(x) = \alpha\lambda x^{\alpha-1}, \alpha > 0, \lambda > 0 \quad (8)$$

$$S(x) = exp(-\lambda x^{\alpha}), \alpha > 0, \lambda > 0 \quad (9)$$

$$E(X) = \frac{\Gamma\left(1+\frac{1}{\alpha}\right)}{\lambda^{\frac{1}{\alpha}}}, \alpha > 0, \lambda > 0 \quad (10)$$

Weibull distribution is considerably flexible. It can explain increasing (for $\alpha > 1$), decreasing (for $\alpha < 1$), or simply a constant hazard rate (for $\alpha = 1$). Since we are going to limit that the hazard rate is always increasing, the value of α must be greater than unity. Therefore, it has a mode equal to $\left(\frac{\alpha-1}{\alpha\lambda}\right)^{\frac{1}{\alpha}}$. By limiting our attention to $x \geq 1$, the hazard rate is a monotone increasing function of both α and λ.

B. Model Construction

The construction of a new distribution as a mixture of several distributions is required under certain circumstances to produce a better fit for the data, as demonstrated in [29]–[32]. The probability density function of the new distribution could be expressed as a weighted sum of probability density functions given by the base distributions, ensuring that the weights are nonnegative real numbers, and their sum equals one. Consequently, the cumulative distribution function, survival function, and raw moments function of the new distribution could also be expressed as the weighted sum of the respective functions given by the base distributions.

In this study, we modified the parameterization of the base distributions to construct a new model that is more interpretable. By denoting X as a random variable that represents a newborn's future lifetime, X's survival function could be expressed as (11).

$$S(x) = \frac{1}{1+R_A+R_S+R_L}\left(\frac{C_1}{x+C_1}\right)^{C_2} + \frac{R_A}{1+R_A+R_S+R_L}\left(\frac{1}{1+\frac{A_2}{A_1^{1+A_2}}x^{1+A_2}}\right) + \frac{R_S\, exp\left(-\left(\frac{x}{(65+S_1)\left(\frac{1+S_2}{S_2}\right)^{\frac{1}{1+S_2}}}\right)^{1+S_2}\right)}{(1+R_A+R_S+R_L)} + \frac{R_L\, exp\left(-\left(\frac{x}{(100+L_1)\left(\frac{1+L_2}{L_2}\right)^{\frac{1}{1+L_2}}}\right)^{1+L_2}\right)}{(1+R_A+R_S+R_L)} \quad (11)$$

The explanations of the notations are provided in the following section.

C. Model Interpretation and Determination of Prior Distributions

In this subsection, we interpret every parameter intuitively and explain how changing their values affects the mortality condition. Based on the explanation and results from previous studies, as discussed in Section I, we determine the prior distribution for the model's parameters. Determination of prior plays a crucial role in the Bayesian procedure as it affects the posterior's complexity and computability and produces reliable results [33]–[37].

1) Weights of Mixing Distribution: Weights of the mixing distribution are determined by the values of R_A, R_S, and R_L. They represent the probability that a newborn will die as an adolescent, a senescent, or a late elderly (who possibly breaks the record of lifespan) compared to the probability that the newborn dies in her/his childhood, respectively. We consider childhood and senescence as the two most important phases in life, so we start our analysis from R_S.

Newborn deaths are the most dominant in childhood mortality. According to World Bank [38], the worldwide lowest mortality rate for an infant in 2018 occurs in Finland, with the rate equal to 1 per 1000 for both sexes. If the adolescence and late elderly phase are abandoned, then we assume that the upper threshold for R_S could be set to 999. Schell et al.[39] listed that assuming childhood ends at the age of 5, its mortality rate in India equals 0.152 for the year 1987. Hence, we could assume that the lower threshold for R_S could be set to $0.152^{-1} - 1 = 5.579$. Setting the threshold range as a 95-percent confidence interval of a lognormal distribution, we obtain the parameters' value of mean $\mu = 4.313$ and standard deviation $\sigma = 1.323$ to construct the prior distribution for R_S.

Next, we consider R_A. We do not have any reliable information to consider accident humps. However, after looking at the shapes of the observed mortality curves across countries and periods, we assume that the mortality rate at the peak of the accident hump will not exceed the mortality rate of a newborn, which dominates childhood mortality. Therefore, exponential distribution with a mean equal to one could be a good choice for the prior distribution of R_A.

The last consideration for getting the weights of mixing is the parameter R_L. We assume that the proportion of the population who die as late elderlies ranges between 0.001 and 0.1. Thus, we set the range of (0.0066, 100) as a 95-percent confidence interval for the prior distribution of R_L, which gives us the value of $\mu = -0.209$ and $\sigma = 2.499$.

It is complicated to directly examine the effects of R_A, R_S, and R_L values on mortality rates. Nevertheless, there is an intuitive way to understand that minimal weights of childhood, adolescence, and senescence mortality contribute to higher life expectancy, also vice versa.

2) Childhood Death: Death in childhood is largely explained by parameters C_1 and C_2, each representing the additive decrease and exponential increase rate of mortality rates in this phase. Former Pareto studies [5] suggest that the values of C_1 and C_2 are mostly close to zero, with the highest logical value being two. Therefore, we choose exponential distribution with its 99-percentile equals two as the prior distribution for both C_1 and C_2. The value of C_2 greater than unity implies that the first moment of X is determinate and finite, as formulated in (12). Therefore, it suggests that life condition in childhood is worse enough to limit the overall lifespan, partly could be due to the parents' behavior and their ability to provide wealth-related resources [40].

$$E(X) = \frac{C_1}{(C_2 - 1)(1 + R_A + R_S + R_L)} + \frac{R_A}{1 + R_A + R_S + R_L}\left(\frac{\pi A_1 \csc\left(\frac{\pi}{A_2 + 1}\right)}{(A_2 + 1)(A_2)^{\frac{1}{A_2}}}\right) + \frac{R_S(65 + S_1)\left(1 + \frac{1}{S_2}\right)}{1 + R_A + R_S + R_L}\Gamma\left(1 + \frac{1}{1 + S_2}\right) + \frac{R_L(100 + L_1)\left(1 + \frac{1}{L_2}\right)}{1 + R_A + R_S + R_L}\Gamma\left(1 + \frac{1}{1 + L_2}\right), C_2 > 1 \tag{12}$$

3) Adolescence Death: Death in adolescence is largely explained by parameters A_1 and A_2. Parameter A1 roughly approximates the peak age of the accident hump. Based on [12] and Chandra and Abdullah [41], the peak of the accident hump is assumed to happen in the age interval of [10, 30]. It is also supported by the fact that Steinberg et al. [42] defined the adolescence phase in equal age intervals. The accident hump was also considered by [43]. Therefore, we choose continuous uniform distribution with domain on the interval [10, 30] as the prior distribution of parameter A_1. A higher value of A1 while keeping other parameters constant will result in lower mortality rates. The exponential increase rate of mortality rate in this phase is denoted by parameter A_2. Looking at the shape of the accident hump, we expect that 1 is a large enough value for A_2, and a smaller value is preferred to prevent overfitting. Consequently, we choose exponential distribution with a mean equaling one as the prior distribution for A_2.

4) Senescence Death: Death in senescence is largely explained by parameters S_1 and S_2. We expect most deaths in this phase to occur after the population becomes elderly and has their pension. Similar to [44], we assume that it happens after 65 years old in current modern life, and it has exceeded 80 in many countries (as also assumed in [45]). In this study, we denote that age as $65 + S_1$. Thus, we choose exponential distribution with the mean of $80 - 65 = 15$ as the prior distribution for S_1. An increased value of S_1 while keeping other parameters constant results in decreased mortality rates. Generally, mortality in this phase is often modeled using the Makeham model. Learning from previous studies [41], [46], and [47], we suggest lognormal distribution with $\mu = 1.278$ and $\sigma = 0.470$ as the prior distribution for S_2, exponential increase rate of mortality rate in this phase so that the goodness of fit in age interval (30, 80] could be as good as the Makeham model.

TABLE I
PRIOR DISTRIBUTIONS FOR THE PARAMETERS

Parameter	Distribution
R_A	Exponential ($\lambda = 1$)
R_S	Lognormal ($\mu = 4.313$, $\sigma = 1.323$)
R_L	Lognormal ($\mu = -0.209$, $\sigma = 2.499$)
C_1	Exponential ($\lambda = 2.303$)
C_2	Exponential ($\lambda = 2.303$)
A_1	Uniform (10, 30)
A_2	Exponential ($\lambda = 1$)
S_1	Exponential ($\lambda = 0.067$)
S_2	Lognormal ($\mu = 1.278$, $\sigma = 0.470$)
L_1	Exponential ($\lambda = 0.1$)
L_2	Lognormal ($\mu = 2.430$, $\sigma = 0.433$)

5) Late Elderlies' Death: Finally, we explain death for late elderlies by parameters L_1 and L_2. Abridged life tables that are constructed by World Population Prospects of the United States [48] group all centenarians in an open age interval. In comparison, complete life tables supplied by the Human Mortality Database group all centenarians with ages over 110 in an open age interval. Even though we do not have any limiting age for our model, we are interested in investigating the maximum age that needs extra attention, which is denoted as $100 + L_1$, as we learned that it is expected to have more centenarians in the future due to better income in the long run [49]. Therefore, we choose exponential distribution with a mean equaling ten as the prior distribution of L_1. A higher value of L_1 with other parameters' values will not change, resulting in a decrease in mortality rates. Chandra and Abdullah [47] forecasted that there would be more centenarians, and human lifespan could exceed age 150 (at their best) in the future. This result is considered possible, but with complete loss of body resilience [50]. Therefore, we choose lognormal distribution with $\mu = 2.430$ and $\sigma = 0.433$ as the prior distribution of L_2, exponential increase rate of mortality rate in this phase, so that the goodness of fit in age interval (80, 230] could be as satisfactory as extrapolating the Makeham model. Prior distributions for all parameters are summarized in Table I. Their parameterization follows Tse [29].

D. Model Fitting

Several algorithms fit the model using the Bayesian method, but Gibbs sampling [51]–[53] is considerably easier with the availability of several software's, such as WinBUGS, OpenBUGS, or JAGS. We found that it was easier for a further calculation to fit the mortality rates instead of the survival probabilities into the model. The value of ${}_tq_x$, the probability that someone aged x will die in *t* years, could be calculated from the survival function by (13).

$$ {}_tq_x = \frac{S(x+t)}{S(x)}, x \geq 0, t > 0 \quad (13)$$

Following previous studies [41] and [47], we put low trust in the data that the variance of the sampling model should be maximized without causing computational error because of the underflow or overflow problem. If we have n values of mortality rates, then the sampling model for each value could be expressed as (14). One important thing to note is that readers must remove a value that exactly equals 1 to fit the model.

$$\left({}_{t_j}q_{x_j} | R_A, R_S, R_L, C_1, C_2, A_1, A_2, S_1, S_2, L_1, L_2\right) \sim Beta\left(1, \frac{S(x_j+t_j)}{S(x_j)-S(x_j+t_j)}\right), j = 1,2,\ldots,n \quad (14)$$

One important thing to note is that we have eleven parameters in this model. Using a complete life table supplied by Human Mortality Database is enough because we have exactly 110 values of complete mortality rates. However, using abridged life tables constructed by World Population Prospects of United Nations [48] means we need bootstrapping practice, as done by Chandra and Abdullah [41], to reduce the sensitivity of prior distribution specifications. By assuming conditional independence on the data, we could construct our posterior joint density of the parameters that is proportional to the product of prior distribution density functions of the parameters and the sampling model. We do not provide its mathematical expression here due to its complexity.

E. Best and Worst Estimate of Newborn Survival Probabilities

As discussed in subsection II.C, the effects of R_A, R_S, and R_L parameters on the estimated survival probabilities of newborns are complicated. However, we could accept that generally, the best condition occurs if there are fewer deaths in childhood, adolescence, and senescence. Therefore, we propose maximizing the RL value, then set the values of R_A and R_S equal to their posterior mean. The worst condition occurs due to death in childhood, adolescence, and senescence. Thus, we propose to minimize the value of R_L, then set the values of R_A and R_S equal to their posterior mean. For the rest, we choose to minimize the values of C_1, A_1, S_1, and L_1, and also maximize the values of C_2, A_2, S_2, and L_2 to calculate our worst estimate and vice versa. Our optimization is based on (100-α)-percent symmetric credible interval of posterior distributions.

III. Results and Discussion

We fitted several data for analyzing our model's performance. We took complete life tables from Human Mortality Database for Swedish males in the year 1751 [54] (which was also considered in [55]), Israeli males in the year 1987 [56], and South Korean females in 2008 [57], also the 4th Indonesian Mortality Table (TMI IV) for both males and females [4]. From each table, we obtained values of q_0, q_1, q_2, …, q_{108}, and q_{109} to fit into the model. We set the 1st 100 iterations for burn-in and the next 2000 iterations for sampling. Even though the number of iterations is considerably small, we considered that this analysis is quite effective in detecting whether the model needs a long time to mix well and/or whether it fits well on the data.

A. Goodness of Fit

Looking at values of Gelman-Rubin $\hat{R}$ statistic for every parameter, stationarity and convergence are achieved as all of them are very close to one. Therefore, we need to look at the plots that compare the actual value to the fitted value of annual mortality rates. Since mortality rates are relatively small, we provide the plot in the natural logarithm form of the values as displayed in Fig. 2, following the approach from Li [58]. A newborn's probability of survival at least to certain ages, simply described as values of newborn survival function, is also plotted in Fig. 3 for every life table. Dashed and solid lines, respectively, represent fitted and actual values.

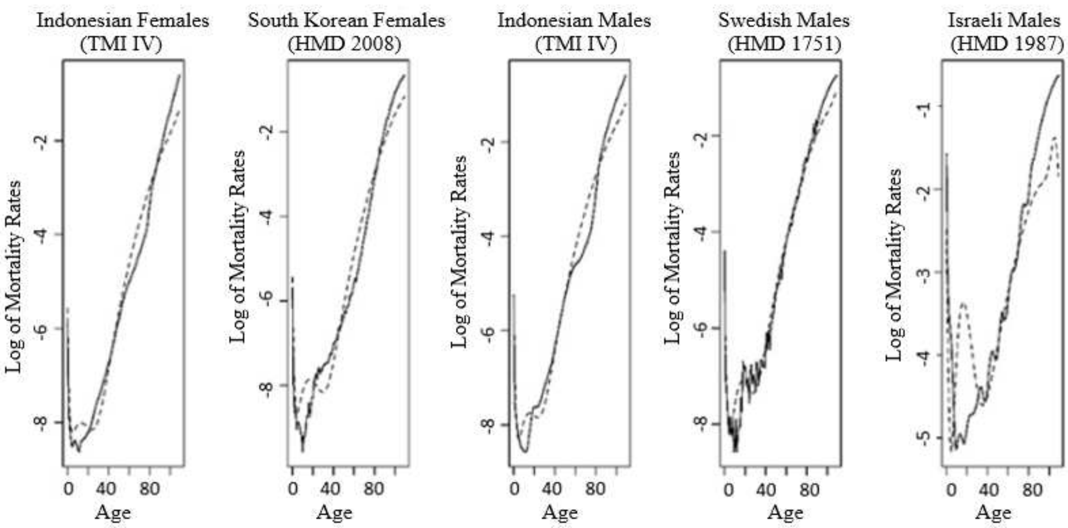

Fig. 2 Natural logarithm form of actual (solid lines) and fitted (dashed lines) annual mortality rates

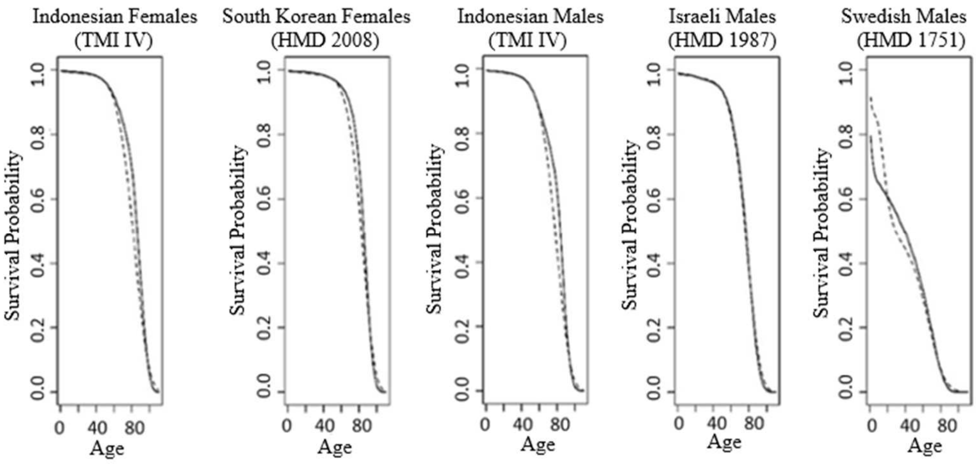

Fig. 3 Actual (solid lines) and fitted (dashed lines) newborn survival function plots.

Fig. 2 and Fig. 3 suggest that the best fit of this model is on the Israeli males' life table for the year 1987. For the rest, fitted models tend to overestimate the mortality rates in early adolescence (age 10 to 20) [59], [60], underestimate in late adolescence and early senescence (age 20 to 50) [61], overestimate in late senescence (age 50 to ≈ 80) and underestimate in late elderlies phase.

Newborn survival probabilities are also overestimated for ages under 80 and underestimated for ages over 80, except for Swedish males. However, a fitted model could estimate the shape of newborn survival functions quite well. Coefficient of determination (R^2) for both annual mortality rates and newborn survival probabilities are also considerably good as all of them exceed 93%, satisfying the criteria set by [62] that a good model should have at least 90% rate of R^2.

B. Determination of Alpha

This section investigates the logical value of α to be later implemented in future works. We calculate the highest possible positive integer for α < 100 so that proportion of actual newborn survival probabilities that is not in the interval formed by the best and worst estimates must be less than fifty percent. The posterior mean of every parameter must also be contained in the interval formed by (100-α)-percent symmetric credible interval of their posterior distribution. Based on our observations of the five life tables we considered in subsection III.A, we suggest α = 14 for future implementations.

C. Model Implementation

Referring to our explanation in Subsection II.C.5, we could set the value of $(100 + L_1)$ as the limiting age. Therefore, we adjust the value of $q_{\lceil 100+L_1 \rceil}$ to equal one and $S(x) = 0$ for $x > \lceil 100+L_1 \rceil$. Subsections III.E and IV.B suggest we have our best and worst estimates of newborn survival probabilities based on an 86% symmetric credible interval of posterior parameter distributions. Furthermore, we calculate annual mortality rates based on the best estimate, fitted values, and worst estimate of newborn survival probabilities by (13). Here we provided an example of how to graduate newborn survival probabilities and annual mortality rates for Indonesian females based on TMI IV [4]. The posterior means of parameters in this model are provided in Table II and were used for the fitted model. We intuitively interpreted the values in Table II as the following. The overall death probabilities for a newborn to have occurred in adolescence, senescence, and late elderlies phase compared to in childhood are 1.680, 158.420, and 2.673, respectively.

TABLE II
THE POSTERIOR MEAN OF THE DISTRIBUTION PARAMETERS

Parameter	Value
R_A	1.68
R_S	158.42
R_L	2.67
C_1	0.30
C_2	0.67
A_1	24.42
A_2	1.17
S_1	19.13
S_2	5.83
L_1	5.17
L_2	17.42

We roughly approximated that the peak of accident hump for Indonesian females based on the TMI IV [4] is around age 24 or 25 (because of A_1 values 24.420), and most deaths in senescence occur around age 84 or 85 (because $65 + S_1$ equals 84.134), and the maximum age that needs extra attention is around 105 or 106 (because $100 + L_1$ values 105.167). Therefore, we set 106 as the limiting age in this case. Based on the guidance discussed in subsections III.E and IV.B, we obtained the 86% symmetric confidence interval lower and upper limits for almost every parameter, excluding R_A and R_S. We arranged the values to construct our best estimate, and the worst estimate with the results are served in Table III.

TABLE III
BEST AND WORST ESTIMATES OF SEVERAL PARAMETERS

Parameter	Best estimate	Worst estimate
R_L	10.403	0.056
C_1	0.795	0.026
C_2	0.208	1.370
A_1	29.471	16.330
A_2	0.490	2.082
S_1	21.260	5.310
S_2	5.310	6.381
L_1	14.833	0.280
L_2	5.487	33.671

From Table III, we could estimate that the overall death probabilities for a newborn as late elderlies compared to a child are in the interval [0.056, 10.403]. Our best estimate is 10.403 as more deaths in the old ages than the young ages mean that we expect their lifespan to be long, and our worst estimate is 0.056 as more deaths in the young ages than old ages mean that we expect their lifespan is considerably short. We also could roughly approximate that the peak of accident hump, most deaths in senescence, and maximum age that needs extra attention occur in age interval [16.330, 29.471], [70.310, 86.260], and [100.280, 114.833]. The reason for putting the best estimate higher than the worst is similar to what we explained for R_L. The value of C_2 is expected to be in the interval [0.208, 1.370], so Indonesian females may have a risk factor in their childhood that limits their age. The best estimate for a complete life expectancy of a newborn is indeterminate, and its worst estimate values 87.49 years. Therefore, we set 101 and 115 as limiting ages for the worst and best estimates, respectively.

The final results in annual mortality rates are not presented here due to space efficiency. Please notice that although best estimates, fitted values, and worst estimates of newborn survival probabilities. S(x) is always sorted in descending order for every certain x; best estimates, fitted values, and worst estimates of annual mortality rates at age x (denoted as q_x) are not always sorted in ascending order for every certain x. In the end, the best estimate, fitted value, and worst estimate of newborns curtate life expectancy values of 82.87, 79.27, and 76.64 years, respectively.

Calculating the annual mortality rates shows that the accident hump is insignificant if we refer to our best estimate of newborn survival probabilities. The overall peak of accident hump occurs in age interval [11, 15] based on the implication of the fitted newborn survival probabilities, and the worst estimate even puts the hump peak at age 10. It is worth noting that the best and worst estimates of A_1 in Table III are only rough approximations, so it is clear to understand why the values differ from real peaks obtained after calculating the annual mortality rates.

IV. CONCLUSIONS

In this study, we proposed a model to graduate mortality rates by implementing a mixture of Pareto, log-logistic, and two Weibull distributions. We adjusted the parameterization so it is easier for users to interpret this model once they know the value of the parameters, and they can set feasible limiting ages for the graduated mortality rates. We also proposed implementing the Bayesian method to fit the mortality rates into the model and calculate best estimates, fitted values, and worst estimates of newborn survival probabilities denoted as S(x). Once S(x) values are obtained, we could calculate implied annual mortality rates (q_x). Implementing the model to several datasets showed satisfactory results, as implied by good graphical fit and high R^2 values.

ACKNOWLEDGMENT

This research is funded by PUTI Q3 2020 research grant from DRPM Universitas Indonesia under Contract No. NKB-1972/UN2.RST/HKP.05.00/2020. We thank Asosiasi Asuransi Jiwa Indonesia for permitting us to use TMI IV in this study. We also acknowledge the editors for spending their valuable time processing this manuscript for IJASEIT.

REFERENCES

[1] D. Dickson, M. Hardy, M. Hardy, and H. Waters, *Actuarial Mathematics for Life Contingent Risks*, 2nd ed. New York: Cambridge University Press, 2018.

[2] "A practitioner's guide to statistical mortality graduation | SOA." https://www.soa.org/resources/tables-calcs-tools/2018-stat-mort-graduation/ (accessed Jan. 03, 2021).

[3] H. Yamazaki, "SMT 2018 (Standard Mortality Table 2018)," Institute of Actuaries of Japan, 2017.

[4] AAJI, "Tabel Mortalitas Indonesia IV," *Asos. Asuransi Jiwa Indones.*, vol. 1, no. October, 2019.

[5] J. Marín-García, M. J. Goldenthal, and G. W. Moe, "Post-genomic view of aging: definitions, theories and observations," in *Aging and the Heart: A Post-Genomic View*, Springer US, 2008, pp. 3–31.

[6] R. Fivaz-Silbermann, *Nouvelles recherches sur l'Ecole de Lausanne*. Geneve, 1976.

[7] L. Heligman and J. H. Pollard, "The age pattern of mortality," *J. Inst. Actuar.*, vol. 107, no. 1, pp. 49–80, 1980.

[8] P. Dellaportas, A. F. M. Smith, and P. Stavropoulos, "Bayesian analysis of mortality data," *J. R. Stat. Soc. Ser. A Stat. Soc.*, vol. 164, no. 2, pp. 275–291, 2001, doi: 10.1111/1467-985X.00202.

[9] S. Mazzuco, B. Scarpa, and L. Zanotto, "A mortality model based on a mixture distribution function," *Popul. Stud. (NY).*, vol. 72, no. 2, pp. 191–200, May 2018, doi: 10.1080/00324728.2018.1439519.

[10] M. Engelman, H. Caswell, E. A.-D. Research, and U. 2014, "Why do lifespan variability trends for the young and old diverge? A perturbation analysis," *ncbi.nlm.nih.gov*, Accessed: Dec. 03, 2020. [Online]. Available: https://www.ncbi.nlm.nih.gov/pmc/articles/pmc4326020/.

[11] M. Bebbington, C. Lai, R. Z.-J. of T. Biology, and U. 2007, "Modeling human mortality using mixtures of bathtub shaped failure distributions," *Elsevier*, Accessed: Aug. 20, 2020. [Online]. Available: https://www.sciencedirect.com/science/article/pii/S0022519306005534.

[12] J. de Beer and F. Janssen, "A new parametric model to assess delay and compression of mortality," *Popul. Health Metr.*, vol. 14, no. 1, Dec. 2016, doi: 10.1186/s12963-016-0113-1.

[13] A. Feckler, M. Low, J. P. Zubrod, and M. Bundschuh, "When significance becomes insignificant: Effect sizes and their uncertainties in Bayesian and frequentist frameworks as an alternative approach when analyzing ecotoxicological data," *Environ. Toxicol. Chem.*, vol. 37, no. 7, pp. 1949–1955, Jul. 2018, doi: 10.1002/etc.4127.

[14] S. C. Smid, D. McNeish, M. Miocevic, and R. van de Schoot, "Bayesian versus frequentist estimation for structural equation models in small sample contexts: A systematic review," *Structual Equ. Model. A Multidiscip. J.*, vol. 27, no. 1, pp. 131–161, Jan. 2020, doi: 10.1080/10705511.2019.1577140.

[15] M. Flor, M. Weiß, T. Selhorst, C. Müller-Graf, and M. Greiner, "Comparison of Bayesian and frequentist methods for prevalence estimation under misclassification," *BMC Public Health*, vol. 20, no. 1, pp. 1–10, Jul. 2020, doi: 10.1186/s12889-020-09177-4.

[16] G. B. King, A. E. Lovell, L. Neufcourt, and F. M. Nunes, "Direct comparison between Bayesian and frequentist uncertainty quantification for nuclear reactions," *Physiscal Rev. Lett.*, vol. 122, no. 23, p. 232502, 2019, Accessed: Jun. 22, 2021. [Online]. Available: https://journals.aps.org/prl/abstract/10.1103/PhysRevLett.122.232502.

[17] M. A. J. S. van Boekel, "On the pros and cons of Bayesian kinetic modeling in food science," *Trends Food Sci. Technol.*, vol. 99, pp. 181–193, 2020, Accessed: Jun. 22, 2021. [Online]. Available: https://www.sciencedirect.com/science/article/pii/S0924224419304170.

[18] M. Safari, N. Masseran, K. I.-P. A. S. M. and, and undefined 2018, "Optimal threshold for Pareto tail modelling in the presence of outliers," *Phys. A Stat. Mech. Its Appl.*, vol. 509, pp. 169–180, 2018.

[19] M. Raschke, "Alternative modelling and inference methods for claim size distributions," *Ann. Actuar. Sci.*, vol. 14, no. 1, pp. 1–19, 2020.

[20] F. Ashkar, I. Ba, and E. Volpi, "Selection between the generalized Pareto and kappa distributions in peaks-over-threshold hydrological frequency modelling," *Hydrol. Sci. J.*, vol. 62, no. 7, pp. 1167–1180, May 2017, doi: 10.1080/02626667.2017.1302089.

[21] H.-H. Kwon, D. Han, and D.-I. Kim, "Bias correction of daily precipitation over South Korea from the long-term reanalysis using a composite Gamma-Pareto distribution approach," *Hydrol. Res.*, vol. 50, no. 4, pp. 1138–1161, 2019, doi: 10.2166/nh.2019.127.

[22] S. Surendran and K. Tota-maharaj, "Effectiveness of log-logistic distribution to model water-consumption data," *J. Water Supply Res. Technol.*, vol. 67, no. 4, pp. 375–383, 2018.

[23] S. Markov, N. Kyurkchiev, A. Iliev, and A. Rahnev, "A note on the log-logistic and transmuted log-logistic models: some applications," *Dyn. Syst. Appl.*, vol. 27, no. 3, pp. 593–607, 2018, doi: 10.12732/dsa.v27i3.9.

[24] N. Kyurkchiev and M. Svetoslav, "A family of recurrence generated sigmoidal functions based on the Log-logistic function: Some approximation aspects," *Biomath Commun.*, vol. 5, no. 1, 2018.

[25] A. Arfeen, K. Pawlikowski, D. McNickle, and A. Willig, "The role of the Weibull distribution in modelling traffic in internet access and backbone core networks," *J. Netw. Comput. Appl.*, vol. 141, pp. 1–22, 2019.

[26] E. E. Elmahdy, "Modelling reliability data with finite Weibull or Lognormal mixture distributions," *Appl Math Inf. Sci*, vol. 11, no. 4, pp. 1081–1089, 2017, doi: 10.18576/amis/110414.

[27] A. Chowdury, "Constitutive modelling and Weibull statistical analysis for the porosity-mechanical property correlations in 3% yittria-stabilized zirconia system," *Int. J. Refract. Met. Hard Mater.*, vol. 70, pp. 246–252, 2018.

[28] S. A. Klugman, H. H. Panjer, and G. E. Willmot, *Loss Models: From Data to Decisions*, 5th ed. New Jersey: John Wiley & Sons, 2019.

[29] Y.-K. Tse, *Nonlife Actuarial Models: Theory, Methods and Evaluation*. New York: Cambridge University Press, 2009.

[30] B. P. Singh, S. Singh, and U. D. Das, "A general class of new continuous mixture distribution and application," *J. Math. Comput. Sci.*, vol. 11, no. 1, pp. 585–602, 2021, doi: 10.28919/jmcs/5227.

[31] E. Williford, V. Haley, L. A. McNutt, and V. Lazariu, "Dealing with highly skewed hospital length of stay distributions: The use of Gamma mixture models to study delivery hospitalizations," *PLoS One*, vol. 15, no. 4, Apr. 2020, doi: 10.1371/journal.pone.0231825.

[32] A. Ickowicz and R. Sparks, "Modelling hospital length of stay using convolutive mixtures distributions," *Stat. Med.*, vol. 36, no. 1, pp. 122–135, 2017.

[33] Q. F. Gronau, A. Ly, and E. J. Wagenmakers, "Informed Bayesian t-Tests," *Am. Stat.*, vol. 74, no. 2, pp. 137–143, Apr. 2020, doi: 10.1080/00031305.2018.1562983.

[34] V. Fortuin, A. Garriga-Alonso, M. van der W.-S. Impacts, and undefined 2021, "Speech enhancement using Bayesian wavenet," *Interspeech*, pp. 2013–2017, 2017, Accessed: Jun. 22, 2021. [Online]. Available: https://www.sciencedirect.com/science/article/pii/S2665963821000270.

[35] A. Gelman, D. Simpson, and M. Betancourt, "The prior can often only be understood in the context of the likelihood," *Entropy*, vol. 19, p. 555, 2017, doi: 10.3390/e19100555.

[36] J. Piironen and A. Vehtari, "On the hyperprior choice for the global shrinkage parameter in the horseshoe prior," *Artif. Intell. Stat.*, pp. 905–913, 2017, Accessed: Jun. 22, 2021. [Online]. Available: https://proceedings.mlr.press/v54/piironen17a.html.

[37] M. C. Axelsen, J. R. M. Jepsen, and N. Bak, "The choice of prior in Bayesian modeling of the information sampling task," *Biol. Psychiatry*, vol. 83, no. 12, p. 60, 2021, doi: 10.1016/j.biopsych.2017.04.021.

[38] World Bank, "Mortality rate, infant (per 1,000 live births) | Data," *World Bank*, 2019. https://data.worldbank.org/indicator/SP.DYN.IMRT.IN (accessed Aug. 12, 2020).

[39] C. O. Schell, H. Rosling, S. Peterson, A. Mia Ekström, and M. Reilly, "Socioeconomic determinants of infant mortality: A worldwide study of 152 low-, middle-, and high-income countries," *Scand. J. Public Health*, vol. 35, no. 3, pp. 288–297, 2007, doi: 10.1080/14034940600979171.

[40] M. M. Williams, B. R. Kemp, K. F. Ferraro, and S. A. Mustillo, "Avoiding the major causes of death: Does childhood misfortune reduce the likelihood of being disease free in later life?," *Journals Gerontol. - Ser. B Psychol. Sci. Soc. Sci.*, vol. 74, no. 1, pp. 170–180, Jan. 2019, doi: 10.1093/geronb/gby039.

[41] C. E. Chandra and S. Abdullah, "Estimating Indonesian complete life table and fair annual pure premium range from abridged life table with Bayesian method and bootstrapping." Under review in a peer-reviewed journal, 2021.

[42] L. Steinberg *et al.*, "Around the world, adolescence is a time of heightened sensation seeking and immature self-regulation," *Dev. Sci.*, vol. 21, no. 2, p. e12532, Mar. 2018, doi: 10.1111/desc.12532.

[43] A. Remund, C. G. Camarda, and T. Riffe, "A cause-of-death decomposition of young adult excess mortality," *Demography*, vol. 55, no. 3, pp. 957–978, Jun. 2018, doi: 10.1007/s13524-018-0680-9.

[44] S. Jafarzadeh, M. R. Golrokhian Sani, N. Mokhtari Amirmajdi, and M. Firouzi, "Evaluation of bilateral vestibular dysfunction in Iranian adults and elderlies by electronystagmography and video head impulse test," *Iran. J. Otorhinolaryngol.*, vol. 31, no. 2, pp. 103–1101, 2019, doi: 10.22038/ijorl.2018.32238.2062.

[45] S. Watanabe *et al.*, "Treatment outcomes of Burr-Hole surgery for chronic subdural hematoma in the elderly living beyond life expectancy: A study comparing cure, recurrence, and complications in patients aged ≥80 years versus ≤79 years," *World Neurosurg.*, vol. 132, pp. e812–e819, Dec. 2019, doi: 10.1016/j.wneu.2019.08.003.

[46] C. W. Jordan, *Society of Actuaries' Textbook on Life Contingencies*. Chicago: The Society of Actuaries, 1991.

[47] S. Chandra, Christian Evan; Abdullah, "Forecasting mortality trend of Indonesian old aged population with Bayesian method." Under review in a peer-reviewed journal, 2021.

[48] United Nations, "World population prospects - population division - United Nations," *Department of Economic and Social Affairs Population Dynamics*, 2020. https://population.un.org/wpp/default.aspx?aspxerrorpath=/wpp/Download/Standard/Mortality/WPP2019_MORT_F17_3_ABRIDGED_LIFE_TABLE_FEMALE.xlsx. (accessed Oct. 02, 2020).

[49] Y. Huang, "Is centenarian rate independent from economy?," *Arch. Gerontol. Geriatr.*, vol. 93, p. 104312, Mar. 2021, doi: 10.1016/j.archger.2020.104312.

[50] T. V. Pyrkov, K. Avchaciov, A. E. Tarkhov, L. I. Menshikov, A. V. Gudkov, and P. O. Fedichev, "Longitudinal analysis of blood markers reveals progressive loss of resilience and predicts human lifespan limit," *Nat. Commun.*, vol. 12, no. 1, p. 2765, Dec. 2021, doi: 10.1038/s41467-021-23014-1.

[51] D. Marcotte and D. Allard, "Gibbs sampling on large lattice with GMRF," *Comput. Geosci.*, vol. 111, pp. 190–199, 2018.

[52] Y. Huang, J. L. Beck, and H. Li, "Bayesian system identification based on hierarchical sparse Bayesian learning and Gibbs sampling with application to structural damage assessment," *Comput. Methods Appl. Mech. Eng.*, vol. 318, pp. 382–411, 2017.

[53] Y. Huang and J. L. Beck, "Full Gibbs sampling procedure for Bayesian system identification incorporating sparse Bayesian learning with automatic relevance determination," *Comput. Civ. Infrastruct. Eng.*, vol. 33, no. 9, pp. 712–730, 2018.

[54] HMD, "Sweden, Total Population, Life Tables (period 1x1), Males," *Human Mortality Database*, 2020. https://www.mortality.org/cgi-bin/hmd/country.php?cntr=SWE&level=1 (accessed Oct. 20, 2020).

[55] F. Colchero and B. Y. Kiyakoglu, "Beyond the proportional frailty model: Bayesian estimation of individual heterogeneity on mortality parameters," *Biometrical J.*, vol. 62, no. 1, pp. 124–135, Jan. 2020, doi: 10.1002/bimj.201800280.

[56] HMD, "Israel, Total Population, Life Tables (period 1x1), Males," *Human Mortality Database*, 2020. https://www.mortality.org/cgi-bin/hmd/country.php?cntr=ISR&level=1 (accessed Oct. 20, 2020).

[57] HMD, "Republic of Korea, Total Population, Life Tables (period 1x1), Females," *Human Mortality Database*, 2020. https://www.mortality.org/cgi-bin/hmd/country.php?cntr=KOR&level=1 (accessed Oct. 20, 2020).

[58] N. Li, "Estimating complete life tables for populations with limited size: From graduation to equivalent construction," *Taylor Fr.*, vol. 24, no. 1, pp. 22–35, Jan. 2019, doi: 10.1080/10920277.2019.1585879.

[59] L. Vu, J. Pulerwitz, B. Burnett-Zieman, C. Banura, J. Okal, and E. Yam, "Inequitable gender norms from early adolescence to young adulthood in Uganda: Tool validation and differences across age groups," *J. Adolesc. Heal.*, vol. 60, no. 2, pp. S15–S21, Feb. 2017, doi: 10.1016/j.jadohealth.2016.09.027.

[60] K. L. Humphreys *et al.*, "Foster care promotes adaptive functioning in early adolescence among children who experienced severe, early deprivation," *J. Child Psychol. Psychiatry Allied Discip.*, vol. 59, no. 7, pp. 811–821, Jul. 2018, doi: 10.1111/jcpp.12865.

[61] Y. Hori, A. Matsumura, T. Namikawa, M. Kato, M. Iwamae, and H. Nakamura, "Comparative study of the spinopelvic alignment in patients with idiopathic lumbar scoliosis between adulthood and adolescence," *World Neurosurg.*, vol. 149, pp. e309–e315, May 2021, doi: 10.1016/j.wneu.2021.02.031.

[62] S. Krivenko, V. Lukin, O. Krylova, and V. Shutko, "Visually lossless compression of retina images," in *2018 IEEE 38th International Conference on Electronics and Nanotechnology, ELNANO 2018 - Proceedings*, Sep. 2018, pp. 255–260, doi: 10.1109/ELNANO.2018.8477459.